Pakistan Veterinary Journal

ISSN: 0253-8318 (PRINT), 2074-7764 (ONLINE)
DOI: 10.29261/pakvetj/2022.058

RESEARCH ARTICLE

Protoscolicidal and Biocompatibility Properties of Biologically Fabricated Zinc Oxide Nanoparticles Using *Ziziphus spina-christi* Leaves

Bushra H Shnawa[1,2], Parwin J Jalil[1,2], Peyman Aspoukeh[2], Daniyal A Mohammed[1] and Donia M Biro[1]

[1]Biology Department, Faculty of Science, Soran University, Kurdistan-Iraq
[2]Scientific Research Centre, Soran University, Kurdistan- Iraq
*Corresponding author: bushra.shnawa@soran.edu.iq

ARTICLE HISTORY (22-190)

Received:	June 15, 2022
Revised:	July 24, 2022
Accepted:	July 27, 2022
Published online:	August 14, 2022

Key words:
ZnO-NPs
Ziziphus Spina-Christi L.
Protoscolicidal
Biocompatibility

A B S T R A C T

The current study presents the green fabrication of zinc oxide nanoparticles (ZnO-NPs) using the leaf extract of *Ziziphus spina-christi* and their protoscolicidal effects and hemocompatibility. The obtained nanoparticles were recognized by Ultraviolet-visible (UV–Vis) spectrometry, X-ray diffraction (XRD), scanning electron microscopy (SEM), and energy-dispersive X-ray spectroscopy (EDX) analysis. The present results confirmed the creation of ZnO-NPs as a spherical shape in SEM with an average particle size of about 83 nm and presented an absorption maximum at 355 nm in the UV-Vis data. EDS analysis confirmed the elemental composition and revealed strong signals for zinc and oxygen. XRD spectrum expressed the hexagonal wurtzite form with an average crystallite size of ~ 31.2 nm. The potential of *in vitro* protoscolicidal efficacy of ZnO-NPs was reported in this paper. The highest antiparasitic activity was at 400 µg / ml of ZnO-NPs after 60 min of the exposure period, with a 100% mortality of the treated protoscoleces. Several morphological alterations were observed on the protoscoleces by optical and scanning electron microscopy. The lysis of RBCs at various doses of ZnO-NPs was significantly less than the positive control, thus proposing its biocompatibility. This investigation suggests that phytochemicals like polyphenols in the extract of this plant act as reducing and stabilizing agents for the synthesis of ZnO-NPs, which showed promising biological activities. Further studies are required to investigate the ZnO-NPs scolicidial effects in the *in vivo* model. The present work's novelty is utilizing *Z. spina-christi* leaves extract as a substantial reducing and capping agent for ZnO-NPs fabrication. In addition, their antiparasitic and hemocompatibility were investigated.

To Cite This Article: Shnawa BH, Jalil PJ, Aspoukeh PK, Mohammed DA, Biro DM, 2022. Protoscolicidal and biocompatibility properties of biologically fabricated zinc oxide nanoparticles using *Ziziphus spina-christi* leaves. Pak Vet J, 42(4): 517-525. http://dx.doi.org/10.29261/pakvetj/2022.058

INTRODUCTION

The Phyto- science arena has significantly contributed to modern medicine. Medicinal plants are the foremost source for managing many health disorders. About 25% of the existing drugs are directly or indirectly derived from plants (Anand *et al*., 2022).

The (ZnO-NPs) are environment-friendly, easy to fabricate, non-toxic, and biocompatible, making them appropriate for biological applications. Moreover, the USA Food and Drug Administration listed ZnO and four other zinc compounds as generally safe materials (FDA, 2015). ZnO is a semiconductor that has a wide bandgap (~3.37 eV) with high binding energy (60 meV) and is one of the essential materials (Alivov *et al*., 2003). ZnO-NPs are of specific importance as they are non-toxic and safe, besides being biocompatible. Moreover, ZnO-NPs have optical, electrical, catalytic and antimicrobial potential (Sirelkhatim *et al*., 2015). Remarkably, ZnO-NPs were proved by previous research as non-toxic to human tissues (Colon *et al*., 2006). Previous investigations have applied the extracts of various plant parts to fabricate ZnO- NPs, where the plant extracts act as capping and stabilizing agents to stabilize the resultant nanoparticles and prevent their agglomeration (Basnet *et al*., 2018, Shnawa *et al*., 2021b).

The tree of *Ziziphus spina-christi* belongs to the botanical family Rhamnaceae. It has been known as "Sedr" in Iraq, and the leaves are traditionally used in folk medicine. Reports have revealed that the leaf extract of this tree has a significant quantity of phytochemical molecules, such as phenols, flavonoids, and tannins.

Moreover, the leaves of this plant were proved to have substantial biological potential because of the presence of a high quantity of polyphenolic compounds (Abdulrahman *et al*., 2022). *Z. spina-christi* (L.) fruits are edible, highly nutritious and rich in vitamin C. Its species are used in folk medicine to treat blisters, chest pains, dandruff, fractures, headaches, and mouth problems. According to El-Shahir *et al*. (2022), there is evidence that the crude extracts and purified chemical components from *Z. spina-Christi* leaves and fruits possess antifungal and antioxidant properties. Another recent investigation recommended applying callus extract of *Z. spina-christi*-prepared ZnO-NPs as beneficial natural antioxidants for health preservation against varied oxidative stress-related to degenerative sicknesses (Lashin *et al*., 2021).

Cystic echinococcosis is a zoonotic disease caused by *Echinococcus granulosus* larval stage. Several investigations designated it an emerging or re-emerging disease with significant medical and economic influences in many countries (Eckert *et al*., 2000; Moro and Schantz, 2009). The surgical operation considers a primary therapeutic technique, but other procedures may play an efficient role in its management (Shnawa *et al*., 2021a). Dissemination of hydatid fluid is a cause of recurrence; therefore, a scolicidal compound is utilized for inactivating the protoscoleces during the surgical operation. However, these scolicidal materials have several adverse impacts (Shi *et al*., 2016). Protoscolices are the target for therapeutic materials to prevent the development of hydatid cysts since they can grow into adult worms in their definitive host or into secondary hydatid cysts in the intermediate hosts. Several protoscolicidal agents were utilized to inactivate the protoscoleces in hydatid fluid. Still, most of them have side effects (Al-Malki *et al*., 2022).

Recently, Jahromi *et al*. (2022) suggested that ethanol and sodium chloride are more reliable protoscolocidal substances for clinical application. Furthermore, Hamad *et al*. (2022) concluded within an in vivo study that the green fabricated Ag-NPs could be considered a novel potential therapeutic choice against cystic echinococcosis.

MATERIALS AND METHODS

Chemicals and materials: The chemical materials, for instance, zinc nitrate hexahydrate ($Zn(NO_3)_2.6H_2O$), sodium hydroxide (NaOH), and eosin dye, were obtained from Sigma-Aldrich, USA. Solvents and chemicals were obtained from Merck without additional purifications. Ascorbic acid and glutaraldehyde (Fisher chemical), phosphate-buffered saline (pH 7.2) (HIMEDIA.India).

Plant collection and preparation of the plant extract: Fresh and healthy leaves of *Z. spina-christi* L. were collected from a tree cultivated in Erbil, Kurdistan - Iraq. Twenty-five grams of fresh leaves of *Z. spina- christi* L. were washed, cut into small pieces, and then heated in 250 mL double distilled water for forty minutes at 80°C. The aqueous extract was filtered through Whatman No. 1 filter paper and kept in the refrigerator for further experiments.

Bio- fabrication of ZnO nanoparticles: A total of 100 mL of *Z. spina-christi L.* leaves extract was added dropwise to 50 mL of zinc nitrate $Zn(NO_3)_2\_6H_2O$ with a magnetic stirring at 80°C for 40 min. The pH was adjusted to alkaline (pH = 12) by adding 1M sodium hydroxide (NaOH). The colour change was observed in the final mixture, signifying the nucleation of ZnO-NPs, as checked by the UV–Vis technique, followed by the formation of some snowy sedimentation. The yellow-brownish-coloured solution confirms the formation of ZnO-NPs. The sediment was separated by centrifugation at 7000 rpm for 30 min, and the solid powder was cleaned with ethanol and distilled water twice to remove impurities and contaminants. Finally, burning was performed in a furnace at 500 °C for two hours. As depicted in Fig. 1, the resultant white-coloured powder was collected and kept for further characterization (Shnawa *et al*., 2021b).

Characterization of Nanoparticles: ZnO nanoparticles were biosynthesized by the aqueous extract of the *Z. spina Christi L* leaves and characterized by several analytical analyses. The formation of ZnO NPs was confirmed by a UV–Vis double-beam spectrophotometer (Super Aquarius). It was scanned from 200–850 nm wavelengths. Field emission scanning electron microscopy (FESEM) (Quanta 4500) was used to inspect the morphology of the obtained nanoparticles. The chemical composition of the synthesized nanoparticles was determined by EDX (energy-dispersive X-ray spectroscopy) achieved in FESEM. The X-ray diffraction (XRD) analysis was performed by a PAN analytical X' Pert PRO (Cu Kα = 1.5406 A) during a scanning ratio of 1°/min in the 2θ range of 20 to 80°. Additionally, particle size was calculated by Debye–Scherrer equation (Talam *et al*., 2012).

Biological applications

Protoscolicidal Activity: Hydatid cysts of *E. granulosus* were collected from the naturally infected liver of sheep from the abattoir in Soran City, Kurdistan -Iraq. The hydatid fluid was aseptically aspirated from the cyst. The collected fluid with protoscoleces was left for 15 minutes to settle the protoscolices. Then, the protoscolices were washed with normal saline. The viability of protoscoleces was detected using a 0.1% aqueous eosin stain. Stained protoscoleces were considered dead. In comparison, the colourless protoscoleces were classified as viable. (Smyth and Barrett, 1980).

The activities of ZnO-NPs were evaluated against the *E. granulosus* parasite as described previously by Jalil *et al*. (Jalil *et al*., 2021). Different concentrations of ultra-sonicated ZnO-NPs, including (50,100, 200, 300 and 400 µg /ml), were used. Briefly, 100 µl of protoscoleces ($5x10^3$ protoscoleces/ml) was added to 2.5 ml of the prepared concentrations. The test tubes were incubated at 37°C for various periods. The mortality percentage was calculated by gently mixing ten µl of 0.1 % eosin with 20 µl of the protoscoleces pellet. The protoscoleces were smeared on a microscopic slide and inspected under an optical microscope after 10 minutes. The percentage of viability was evaluated by counting 100 protoscoleces from each treatment. Normal saline (0.9% NaCl) was considered a negative control, and 5% NaCl was positive (Shnawa *et al*., 2017; Jalil *et al*., 2021). The experiment

was repeated in triplicate. The following formula determined the viability percentage of the protoscoleces by the eosin exclusion technique:

Viability of protoscoleces = (No of viable protoscoleces / Total No. of protoscoleces) × 100

For Scanning electron microscopy analysis, 100 µl of treated protoscoleces with ZnO-NPs and control one were processed as described previously by Verma *et al*. (2014) and Shnawa *et al*. (2017). Briefly, the parasite was washed once in phosphate buffer (PBS) pH 7.2 and fixed in 2.5% glutaraldehyde for 24 h at room temperature. Then the specimens were dehydrated by sequential dipping in increasing ethanol concentrations (30%–100%) and were finally air-dried in a sterilized hood. They were then sputter-coated with gold and inspected by FESEM (Quanta 4500) SEM operating at 15 kV.

Blood compatibility of ZnO-NPs: Hemolysis tests using red blood corpuscles (RBCs) were performed to assess the hemolytic ability of ZnO-NPs. An amount of 4 mL of human blood from healthy volunteers was collected in ethylene diamine tetraacetic acid anticoagulant tubes. The process was performed with formal bioethics approval. The blood was centrifuged at 1500 rpm for 10 minutes. After centrifugation, both the buffy coat and plasma were removed from the supernatant, and the pellet was washed with PBS triplicate. The RBCs were diluted to 8 ml with PBS buffer. Then, 200 µL of the diluted RBC suspension was added to 800 µL of the various concentrations of ZnO-NPs suspension in Phosphate buffer saline, PH 7.4 (PBS). The mixture was incubated for 1 hour at 36 C. The supernatant was collected. A UV-vis spectrophotometer measured the released haemoglobin from the supernatant at a wavelength (570 nm). Sterilized PBS and deionized water were utilized as negative control and positive controls, respectively (Taaca and Vasquez, 2018). The percentage of hemolysis was calculated using the following formula:

Hemolysis % = [(Specimens absorbance - Negative control absorbance) / (Positive control absorbance- Negative control absorbance)] × 100

(Chen *et al*., 2015).

Statistical analysis: All experiments were performed in triplicate, and the results are presented as mean±SE. The data were analyzed by GraphPad Prism software version 8. The one-way analysis of variance (ANOVA) and Tukey's tests were performed for multiple comparisons. The significance of the difference was 5% ($p < 0.05$). The inhibition concentration (IC50) values were calculated from linear regression analysis using Microsoft Office Excel 2016.

RESULTS

The present work showed the production of ZnO-NPs by changing the colour of the mixture to yellow after mixing *Z. spina christi* leaves extract with zinc nitrate, which indicates the formation of ZnO-NPs.

Characterization of Green Synthesized ZnO-NPs

UV–Vis analysis of the plant extract and ZnO-NPs: Fig. 2, A depicts the UV-Vis images of the *Z. spina christi* plant leaves extract absorption; the peaks seemed to be around 270 and 320 nm.

Fig. 2B shows the UV-Vis spectrum of the biosynthesized ZnO-NPs. The ZnO-NPs showed an absorbance spectrum at 355 nm in UV–visible spectroscopy, which is an excellent indicator of the formation of ZnO nanoparticles. The following straight transform formula has been used to determine the direct band gap energy (Eg) for the biosynthesized NPs.

$$\alpha h\vartheta = A(h\vartheta - E_g)^n$$

Where α is the optical-absorption parameter, $h\vartheta$ is the photon's energy; *Eg* is the Direct bandgap, *A* is a constant and the power n is influenced by the type of optical transition that predominates. The best choice for n in the applied method is (1/2). The direct bandgap equals 3.02 eV for ZnO- NPs, as shown in Fig. 2B.

Morphological study: To investigate the surface morphology of the biogenic prepared ZnO- NPs, the scanning electron microscope (SEM) has been used, as shown in Fig. 3a. It is evident from the Figure that there are a few agglomerations between the nanoparticles, and also, most of the nanoparticles are spherical. Fig. 3b depicts that most nanoparticles are distributed between 70 and 80 nm with a mean size of 83nm.

X-ray diffraction (XRD): The X-ray diffraction (XRD) pattern of synthesized ZnO nanoparticles is shown in Fig. 3C. The 2theta degree of scanning has been set between 20 to 80. It approved the crystallinity of prepared nanoparticles. The peaks at theta 31.76°, 34.39°, 36.24°, 47.51°, 56.59°, 62.81°, 66.37, 67.92°, 69.07, 72.49°, and 76.94° can be allocated to the (010), (002), (011), (012), (110), (013), (020), (112), (021), (004) and (022) planes, respectively.

It can be seen from Fig. 3C that all the diffraction peaks were indexed to a hexagonal Wurtzite form of ZnO-NPs (ICSD Card no. 98-018–0051). Moreover, there is no additional peak in the XRD patterns, indicating no impurity observed. The crystallite size of prepared nanoparticles could be calculated by studying the full width at half the maximum (FWHM) value of the XRD pattern. By using the Debye–Scherrer equation:

$$D = \frac{0.95\lambda}{\beta_D cos\theta}$$

The D is the average crystallite size (diameter), λ is the wavelength of the incident X-ray (0.154 nm), θ is the Bragg's angle and β_D It is full width at half maximum (FWHM). Debye–Scherrer's equation is an approximate conviction suitable only for spherical and semispherical particles (Speakman, 2014). From the above equation, the average crystallite size is measured to be ~ 31.2 nm, and the average FWHM is equal to 0.3292, offering a high-quality ZnO nanoparticle structure.

EDX and Elemental Mapping: Fig. 4A illustrates the pureness of ZnO-NPs using energy-dispersive x-ray spectroscopy (EDX) analysis. The EDX data confirms the presence of nickel and oxygen atoms in the sample while exhibiting the Zn and O peaks free of other impurities. Also, the chemical elements of ZnO-NPs consisted of 79.5% mass of zinc and 20.4 % oxygen which proved the purity of the biosynthesized ZnO-NPs. The ratio of atomic

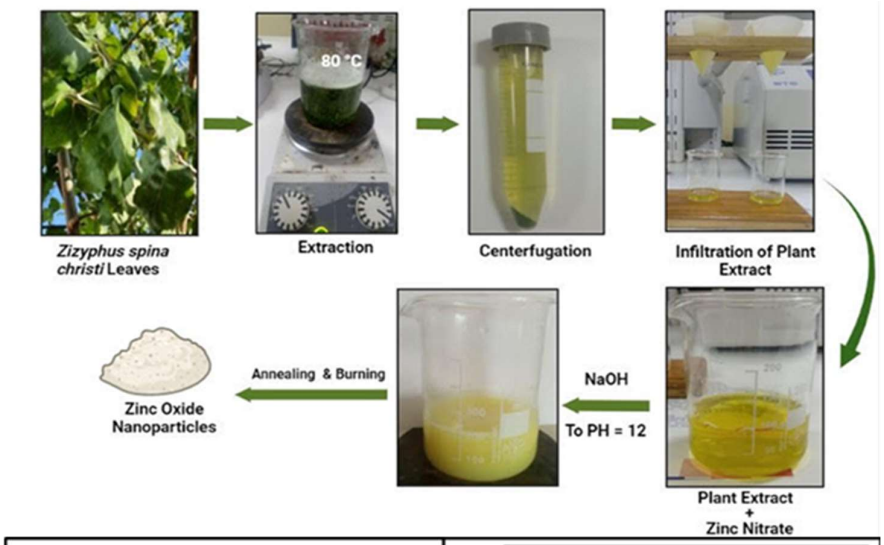

Fig. 1: Flow chart illustrating ZnO-NPS biosynthesis from *Z.spina Christi* leaves extract.

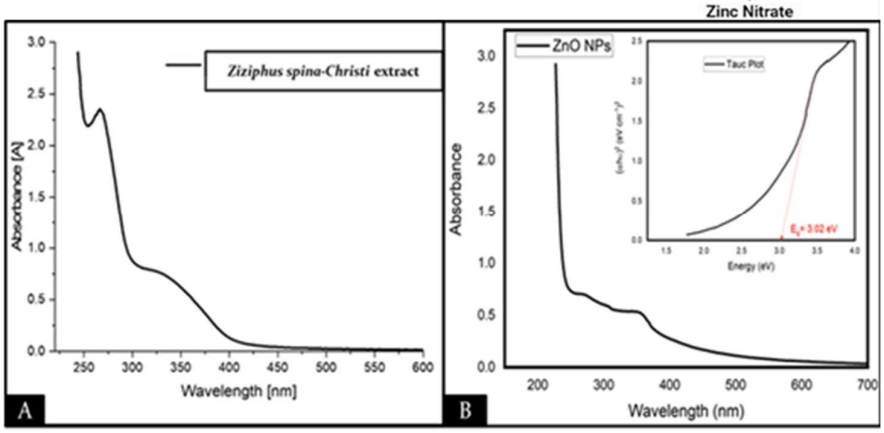

Fig. 2: A. The UV-Vis absorption spectrum of the plant extract of *Z. Spina Christi:* **B.** Depicts the UV-Vis spectrum of the biosynthesized ZnO-NPs

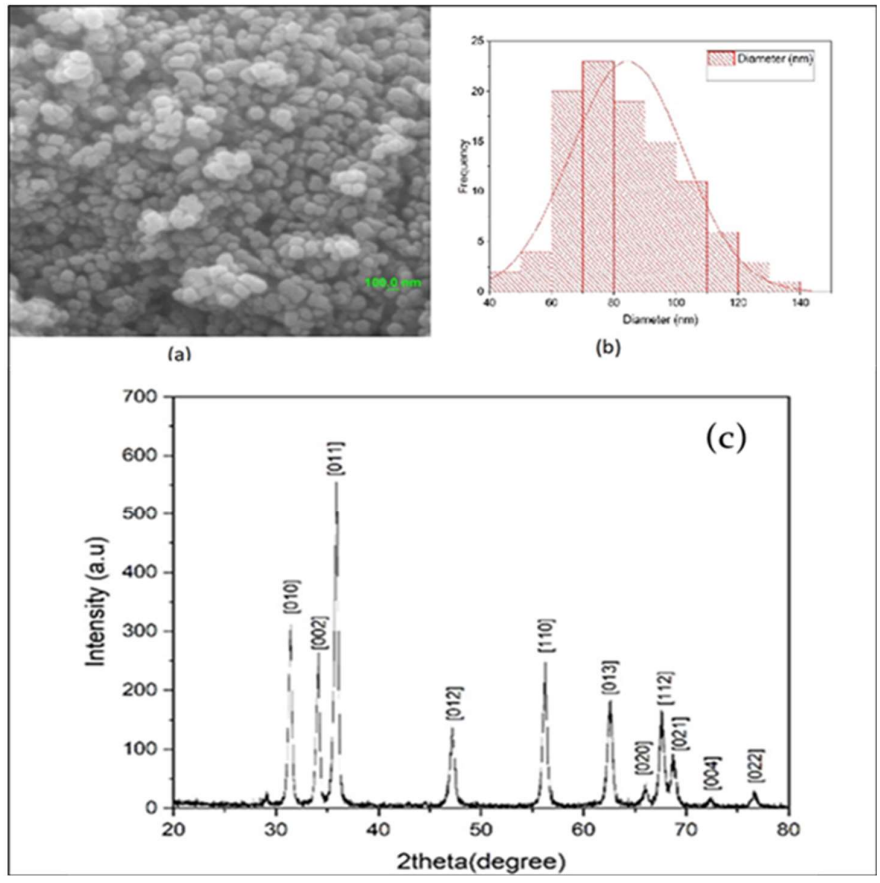

Fig. 3: (a) Scanning electron microscopy image of ZnO -NPs and (b) Histogram showing ZnO-NPs size distribution. (c) Shows the XRD pattern of the green prepared ZnO-NPs.

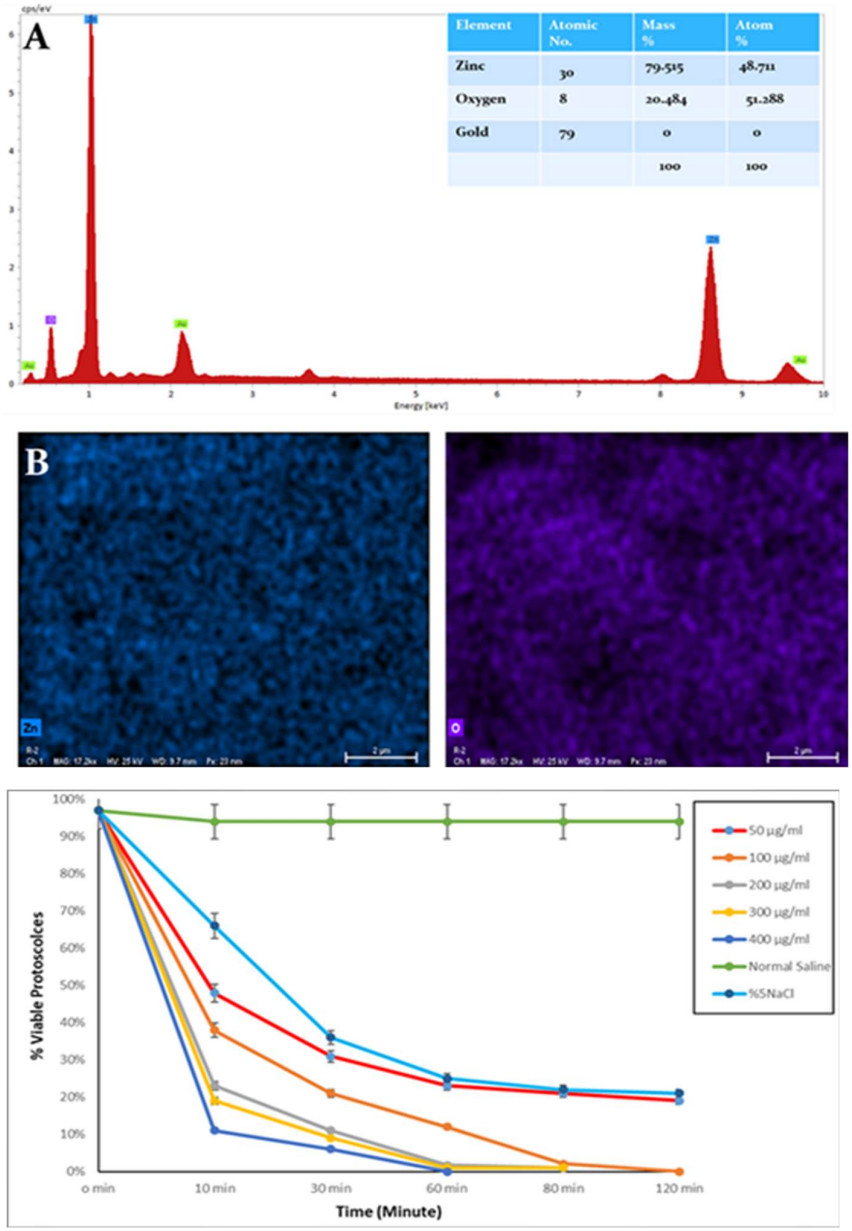

Fig. 4: A. EDX analysis of the biosynthesized ZnO-NPs. **B.** Elemental composition distribution of the biosynthesized ZnO-NPs

Fig. 5: Loss of viability of *E. granulosus* protoscolices during in vitro ZnO-NPs treatment

percentages of Zn to O is 0.95. Additionally, the presence of Au in the EDX spectrum is related to the coating of ZnO-NPs with a thin layer of gold to enhance the quality of the image. Fig. 4B depicts the elemental mapping of ZnO-NPs, which contain Zinc and oxygen distribution with almost no impurity. The X-ray diffraction peaks, SEM micrographs and EDX results show that high-quality ZnO nanoparticles were formed without the impurity or other secondary residues

Protoscolicidal activity of ZnO-NPs: The *in vitro* effects of ZnO-NPs against *E. granulosus* protoscoleces were studied by light microscopy and Scanning electron microscopy. The synthesized ZnO-NPs had a significant scolicidal impact. The 400, 300 and 200 µg /ml nanoparticles exhibited more immediate effects. It caused damage to the protoscoleces (100% mortality) after 60 minutes of treatment, as depicted in Fig. 5. They were followed by the 100 µg /ml ZnO-NPs that caused the parasite's death after 80 minutes of incubation.

A clear attachment of the nanoparticles to the parasite led to the loss of hooks, blebs formation, and irreversible tissue vacuolation, resulting in death compared to the untreated control protoscoleces incubated in the normal saline, as shown in Fig. 6.

The protoscolices of the control group displayed no ultrastructural changes and appeared intact, as shown in Fig. 7A&B; in contrast, the treated parasite showed intensive and dense attachment of the ZnO-NPs, indicating high affinity between the protoscoleces and the nanoparticles; no free nanoparticles were detected around the parasite, as depicted in Fig. 7C &D. The treated protoscolices showed ultrastructural damage. The tegument seemed to be the primary site of injury. Disruption of tegumental integrity results in osmoregulatory damage and contraction of the soma region. Also, other alterations were observed, such as the aggregation and attachment of the protoscoleces, rostellar disorganization and hooks shedding. Moreover, some evaginated protoscoleces expressed contraction of the soma region as in Fig. 7D.

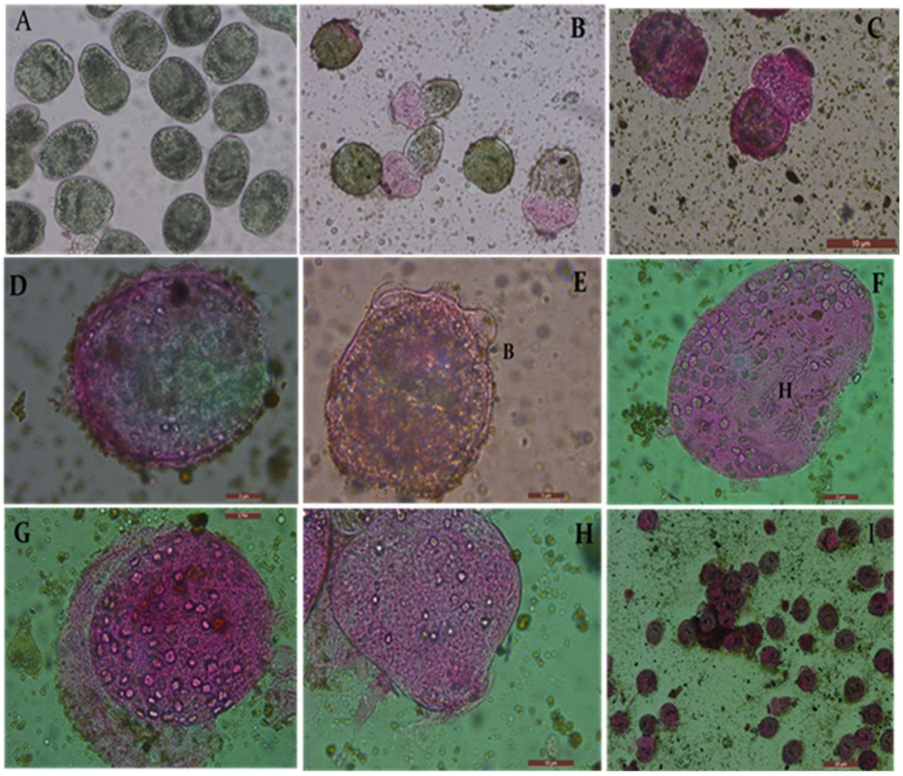

Fig. 6: Protoscoleces by light microscopy: (A) Viable control protoscoleces (B) Partially stained evaginated protoscoleces with eosin indicated their death. (C) Dead invaginated and evaginated protoscoleces treated with ZnO-NPs and stained with eosin indicated their death. (D) Tegumental digitiform structures were observed at the outer tegument of protoscolex treated with ZnO-NPs. (E) Dead-treated protoscolex with bleb (B) formation and loss of parasite integrity. (F) Dead protoscolex presents hooks (H) disorganization. (G) and (H) Dead protoscoleces showed tegumental damage and hooks loss. (I) Dead protoscoleces which treated with ZnO-NPs after one hour of exposure.

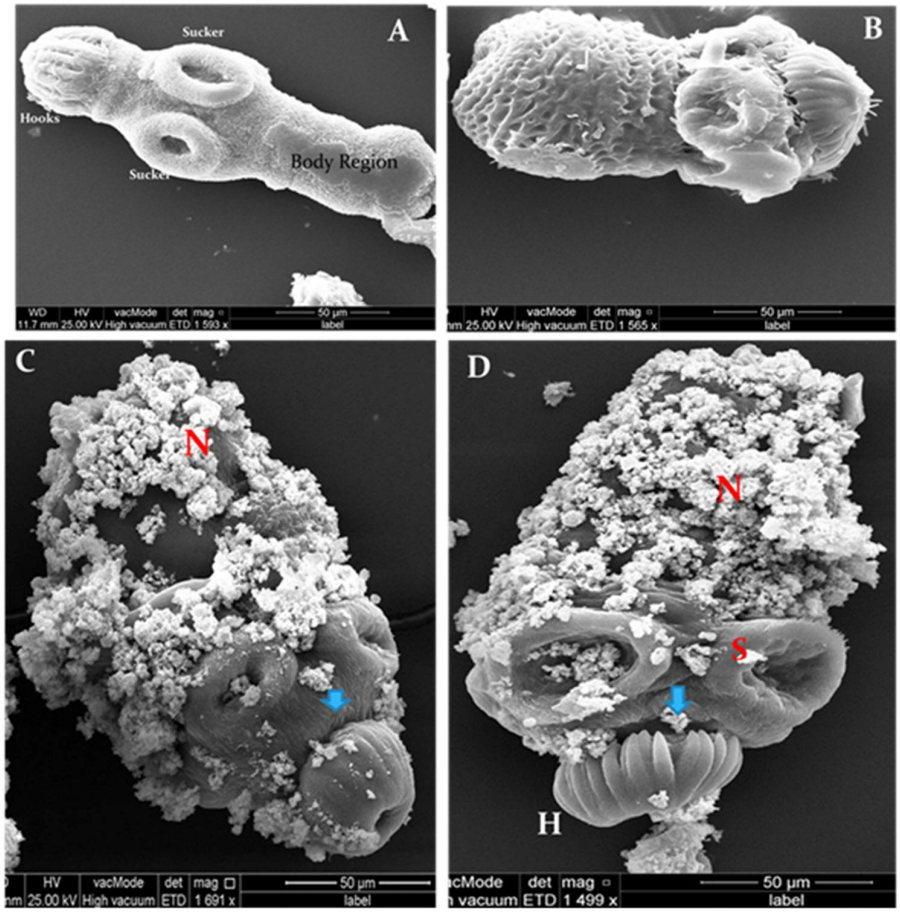

Fig. 7: Protoscolices by SEM: (A) and (B) Evaginated control protoscoleces; Body Region, Suckers (S); Hooks (H). (C) Shows treated evaginated protoscoleces incubated with (300 µg /ml) ZnO-NPs covered with the NPS as a white coloured (N); the arrow indicates the soma region. (D) displays evaginated treated protoscolex with ZnO-NPs, shows contraction of soma region (arrow) And disorganization of rostellar hooks (H) compared to (C) and presence of tegumental and suckers change; Hooks (H), suckers (S).

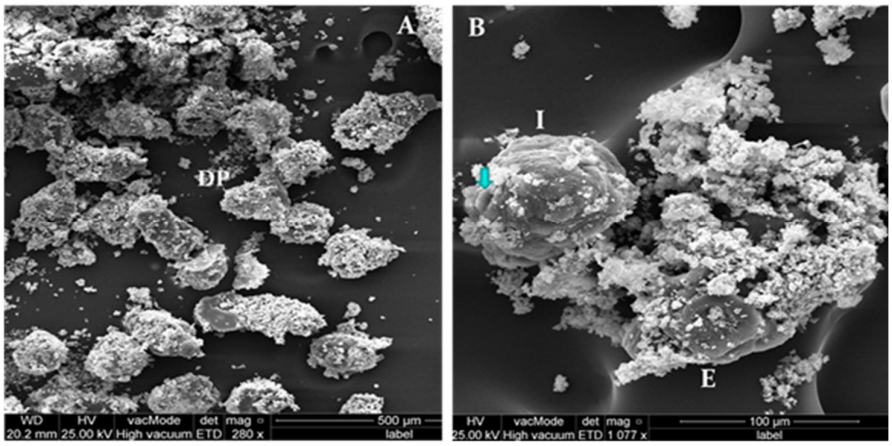

Fig. 8: Protoscolices incubated with ZnO-NPs (400 µg/mL) during an hour of treatment; (A) Aggregation and attachment of protoscoleces with each other with tegumental damage and changes (DP). (B) Invaginated protoscolex (I) displays tegumental changes and blebs formation(arrow). Also, evaginated protoscolex (E) showed deformation of morphology with the accumulation of nanoparticles.

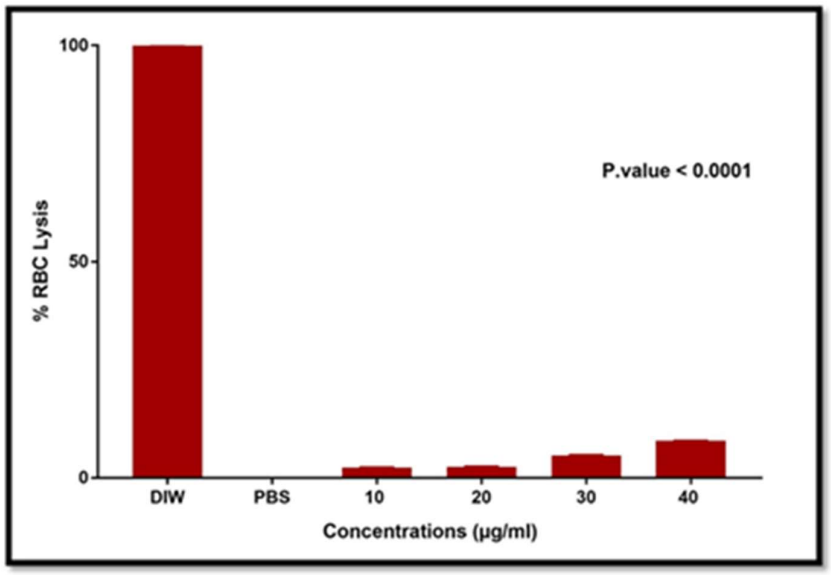

Fig. 9: Effects of different concentrations of ZnO-NPs on RBCs lysis compared to the positive and negative controls. DW: Distilled water, and PBS: Phosphate buffer saline.

Fig. 8. A. Protoscolices incubated with 100 µg/ml Zn-ONPs exhibited the production of blebs on the parasite tegument as in Fig. 8.B.

Blood compatibility of ZnO-NPs: The hemolytic activity test is valuable for quick preliminary toxicity evaluation. The hemolysis experiment was performed and compared with PBS as a negative and double-distilled water as positive controls. The hemolytic activity of ZnO-NPs displayed dose-dependent activity.

The lowest concentration (10 µg /ml) of ZnO-NPs induced 2.3±0.029% hemolysis, followed by 2.5±0.081 % for 20 µg/ml and 5.1±0.085 % for 30 µg /ml. At 40 µg/mL concentration of ZnO-NPs, it caused 8.5±0.028% hemolysis. Lysis of RBCs at different concentrations of ZnO-NPs was significantly ($P \leq 0.05$) less than the positive control value, as displayed in Fig. 9. The present finding proposed that the bio-fabricated ZnO-NPs from *Z. spina-christi* leaves were biocompatible at these tested concentrations.

DISCUSSION

The present work revealed the production of ZnO-NPs by changing the colour of the mixture to yellow after mixing *Z. spina christi* leaves extract with zinc nitrate, which indicates the formation of ZnO-NPs. This change agrees with several previous investigations that reported the appearance of yellow colour as an indicator for ZnNps synthesis (Santhoshkumar *et al*., 2017; Naseer *et al*., 2020; Lashin *et al*., 2021).

The plant extract showed two peaks by UV-Vis. These two peaks are associated with the leaf's phytochemicals related to cinnamoyl and benzoyl phenolic compounds. They would be responsible for the biosynthesis of metallic and metal oxide nanoparticles. Moreover, Singh *et al*. (2019) pointed out that the phenolic compounds expressed adsorption between 320 to 380.

Another study proved that the leaf extract of *Z. spina-christi* was rich in Polyphenols and flavonoids (Almeer *et al*., 2018). There is new evidence that polyphenols are a novel precursor for the green synthesis of ZnO-NPs (Kokabi and Nejad Ebrahimi, 2021). Therefore, according to these facts and the results of this study, *Z. spina-christi* leaves extract act as an effective reducing and capping agent for ZnO-NPs fabrication.

Z. spina christi leaves contain several chemical constituents, including polyphenols, saponins, and tannins, which present higher DPPH radical scavenging activity due to these organic materials (Abalaka *et al*., 2011).

The ZnO-NPs showed absorbance spectra at 355 nm in UV–visible spectroscopy, which is an excellent indicator of the formation of ZnO nanoparticles. The maximum absorption peak for ZnO-NPs ranges from 300 to 380 (Pai *et al*., 2019). A similar UV-vis absorption spectrum of ZnO-NPs was recorded by Talam *et al*. (2012) as an absorption band at 355 nm related to ZnO nanoparticles. The UV–Vis findings revealed no absorption band around 500 nm, indicating the purity of ZnO-NPs from the ionized oxygen. Also, the present results agree with previously published articles (Safawo *et al*., 2018; Chitradevi *et al*., 2019). Once the green fabricated microwave-assisted ZnO-NPs were characterized. The results showed that ZnO-NPs contain hexagonal wurtzite and are represented by a well-defined spherical-like morphology with an outstanding band gap (2.70 eV) (Alharthi *et al*., 2021).

Surgery remains the superior therapeutic choice for *E. granulosus* disease, but other procedures also play a vital role in disease management (Anand *et al*., 2012). Many scolicidal agents are tested to inactivate the protoscoleces during surgery; all scolicidal materials possess adverse influences. For example, nowadays, hypertonic saline is globally used as scolicidal agent. However, it can induce hypernatremia, convulsions, intracranial bleeding, necrosis, and myelinolysis (Adas *et al*., 2009; Shi *et al*., 2016). Therapeutic of cystic echinococcosis still depends on benzimidazole. This drug exhibited severe adverse effects such as leucopenia, alopecia, hepatotoxicity, and thrombocytopenia. Therefore, novel compounds must be explored due to the unavailability of effective treatment for cystic echinococcosis (Shnawa, 2018).

Pérez-Serrano *et al*. (1994) assumed that loss of rostellar hooks and development of blebs are stress responses induced by any harmful event in protoscoleces. Comparable nanoparticle-induced damage was detected on protoscoleces treated with green synthesized AgNPs and ZnO-NPs in other investigations within in vitro and *in vivo* models (Shnawa *et al*., 2021b; Jalil *et al*., 2021; Hamad *et al*., 2022). Moreover, Hu *et al*. (2011) mentioned some drug-induced apoptosis of *E. granulosus* protoscoleces and proved the presence of a CED-3-like apoptosis gene in the protoscoleces. Therefore, apoptosis is a possible mechanism for the action of the ZnO-NPs. The antiparasitic activity of the biosynthesized NPs was related to their high surface area, which led to additional mechanical, chemical, electrical, optical, magnetic, electro-optical and magneto-optical characteristics that differed from their original ones (Whitesides, 2005).

Recently, Shakibaie *et al*. (2022) concluded in an in vitro study that the combination of ZnNPs with albendazole showed potent scolicidal effects. Moreover, Zaheer *et al*. (2021) pointed out that the green synthesized ZnO-NPs are an effective, safer, and eco-friendly option against *Hyalomma* ticks. Bajwa *et al*. (2022) revised the role of NPs in parasitic infection management and summarized that gold and silver have significant effects against different parasites. These NPs target the parasites by several mechanisms, including the destruction of membranes, DNA damage, inhibition of protein synthesis, and free radical action.

The tegument of cestodes has a critical role in the physiology of these parasites, being involved in nutrient absorption, defence mechanisms against the host immunity, and excretion besides ionic transmission. Previous studies documented similar ultrastructural alteration in the protoscoleces incubated with different nanoparticles, plant extracts, and drugs. For instance, the AgNPs (Jalil *et al*., 2021), Scorpion venom (Al-Malki *et al*., 2022), Flubendazole (Elissondo *et al*., 2006), *Cyperus rotundus* extracts (Shnawa, 2017), and Chenodeoxycholic acid (Shi *et al*., 2016).

Also, studies proved the manifestation of the apoptosis process and showed the existence of a CED-3-like apoptotic gene in *E. granulosus* protoscoleces (Hu *et al*., 2011; Al-Malki *et al*., 2022).

The present finding proposed that the bio-fabricated ZnO-NPs from *Z. spina-christi* leaves were biocompatible at the tested concentrations. Luna-Vázquez-Gómez *et al*. (2021) mentioned that according to the American Society for Testing and Materials, less than 5% of hemolysis is considered null, more than this limit, and up to 10% is proposed as low. Hemolysis characterizes the damaged integrity of the erythrocyte membrane, leading to haemoglobin release (ASTM, 2013). Moreover, ZnO-NPs are a multifunctional element which widely used in many applications, such as feed supplements in the animal industry (Mohd Yusof *et al*., 2019).

Conclusions: This study revealed that the *Z. spina-christi* L. leaves extract is an effective reducing and capping agent for the fabrication of ZnO-NPs for the first time and is reported as a sustainable resource; it exhibited critical biological properties. Characterization of ZnO-NPs was accomplished by UV–vis, XRD, SEM and EDX; the results proved their crystallinity and purity. The obtained ZnO-NPs nanoparticles are stable and spherical in SEM with an average particle size of about 83 nm. Also, the purity and elemental percentages of ZnO-NPs were documented by EDX analysis. The prepared nanoparticles exhibited potent in vitro scolicidal effects.

Moreover, ZnO-NPs had low toxicity on the erythrocytes and appeared hemocompatible. Despite the promising findings, more research is needed to clarify the possible mechanism of action of ZnO-NPs against the protoscoleces of *E. granulosus.*

Authors contribution: The research work was performed by Jalil PJ, Aspoukeh P, Mohammed DA and Biro DM Shnawa BH designed and supervised the study. All authors discussed the results and contributed to the final manuscript.

REFERENCES

Abalaka M, Mann A and Adeyemo SO, 2011. Studies on in-vitro antioxidant and free radical scavenging potential and phytochemical screening of leaves of Ziziphus mauritiana L. and Ziziphus spina- christi L. compared with Ascorbic acid. J Med Genet Genomics 3:28-34.

Abdulrahman M, Zakariya A, Hama H, *et al*., 2022. Ethnopharmacology, Biological Evaluation, and Chemical Composition of Ziziphus spina christi (L.) Desf.: A Review. Adv Pharmacol Pharm Sci 2:1-36.

Adas G, Arikan S, Kemik O, *et al*., 2009. Use of albendazole sulfoxide, albendazole sulfone, and combined solutions as scolicidal agents on hydatid cysts (in vitro study). World J Gastroenterol 15:112-6.

Al-Malki ES, Aljedaie MM, Amer OS, *et al*., 2022. Scorpion crude venom induced apoptosis and structural changes of *Echinococcus granulosus* protoscolices. J King Saud Univ Sci 34:101937.

Alharthi M N, Ismail I, Bellucci S, *et al*., 2021. Biosynthesis Microwave-Assisted of Zinc Oxide Nanoparticles with *Ziziphus jujuba* Leaves Extract: Characterization and Photocatalytic Application. Nanomaterials (Basel)11:1682.

Alivov YI, Kalinina E, Cherenkov A, *et al*., 2003. Fabrication and characterization of n-ZnO/p-AlGaN heterojunction light-emitting diodes on 6H-SiC substrates. Appl Phys Lett 83:4719-21.

Almeer RS, El-Khadragy MF, Abdelhabib S, *et al*., 2018. *Ziziphus spina-christi* leaf extract ameliorates schistosomiasis liver granuloma, fibrosis, and oxidative stress through downregulation of fibrinogenic signalling in mice. PLoS One 13:e0204923.

Anand U, Tudu CK, Nandy S, *et al*., 2022. Ethnodermatological use of medicinal plants in India: From ayurvedic formulations to clinical perspectives - A review. J Ethnopharmacol 284:114744.

ASTM 2013. Standard test method for analysis of hemolytic properties of nanoparticles. ASTM International West Conshohocken, PA.

Bajwa HUR, Khan MK, Abbas Z, *et al*., 2022. Nanoparticles: Synthesis and their role as potential drug candidates for the treatment of parasitic diseases. Life (Basel) 12:750.

Basnet P, Inakhunbi Chanu T, Samanta D *et al*., 2018. A review on bio-synthesized zinc oxide nanoparticles using plant extracts as reductants and stabilizing agents. J Photochem Photobiol B 183:201-21.

Chen LQ, Fang L, Ling J, *et al*., 2015. Nanotoxicity of silver nanoparticles to red blood cells: size dependent adsorption, uptake, and hemolytic activity. Chem Res Toxicol 28:501-9.

Chitradevi T, Jestin Lenus A and Victor Jaya N, 2019. Structure, morphology and luminescence properties of sol-gel method synthesized pure and Ag-doped ZnO nanoparticles. Mater Res Express 7 015011

Colon G, Ward BC and Webster TJ, 2006. Increased osteoblast and decreased Staphylococcus epidermidis functions on nanophase ZnO and TiO2. J Biomed Mater Res A 78:595-604.

Eckert J, Conraths FJ and Tackmann K, 2000. Echinococcosis: an emerging or re-emerging zoonosis? Int J Parasitol 30:1283-94.

Elissondo M, Dopchiz M, Ceballos L, *et al*., 2006. In vitro effects of flubendazole on *Echinococcus granulosus* protoscoleces. Parasitol Res 98:317-23.

El-Shahir AA, El-Wakil DA, Abdel Latef AAH, *et al*., 2022. Bioactive Compounds and Antifungal Activity of Leaves and Fruits Methanolic Extracts of *Ziziphus spina-christi* L. Plants 11:746

FDA US 2015. Select committee on GRAS substances (SCOGS) opinion: tannic acid (hydrolyzable gallotannins). GRAS substances (SCOGS) database.

Hamad SM, Shnawa BH, Jalil PJ, *et al*., 2022. Assessment of the Therapeutic Efficacy of Silver Nanoparticles against Secondary Cystic Echinococcosis in BALB/c Mice. Surfaces 5:91-112.

Hu H, Kang J, Chen R, *et al*., 2011. Drug-induced apoptosis of Echinococcus granulosus protoscoleces. Parasitol Res 109: 453-9.

Jahromi KF, Rafiei A, Rahdar M, *et al.,* 2022. Evaluation of the protoscolicidal effectiveness of hypertonic saline, silver nitrate, Ethanol, Using Sponge Pad Method and Injecting into Fertile Hydatid Cysts. Iran J Parasitol 17:223-30.

Jalil PJ, Shnawa BH and Hamad SM, 2021. Silver Nanoparticles: Green synthesis, characterization, blood compatibility and protoscolicidal efficacy against *Echinococcus granulosus*. Pak Vet J 41:393-9.

Kokabi M and Nejad Ebrahimi S, 2021. Polyphenol Enriched Extract of Pomegranate Peel; A Novel Precursor for the Biosynthesis of Zinc Oxide Nanoparticles and Application in Sunscreens. Pharm Sci 27:102-10.

Lashin I, Hasanin M, Hassan S, *et al*., 2021. Green biosynthesis of zinc and selenium oxide nanoparticles using callus extract of Ziziphus spina-christi: characterization, antimicrobial, and antioxidant activity. Biomass Conv Bioref https://doi.org/10.1007/s13399-021-01873-4

Luna-Vázquez-Gómez R, Arellano-García ME and García-Ramos JC, 2021. Hemolysis of Human Erythrocytes by Argovit™ AgNPs from Healthy and Diabetic Donors: An In Vitro Study. Materials 14:2792.

Mohd Yusof H, Mohamad R and Zaidan UH, 2019. Microbial synthesis of zinc oxide nanoparticles and their potential application as an antimicrobial agent and a feed supplement in animal industry: a review. J Animal Sci Biotechnol 10:57.

Moro P and Schantz PM, 2009. Echinococcosis: a review. Int J Infect Dis 13:125-33.

Naseer M, Aslam U, Khalid B and Chen B, 2020. Green route to synthesize Zinc Oxide Nanoparticles using leaf extracts of Cassia fistula and Melia azadarach and their antibacterial potential. Sci Rep 10:9055.

Pai S, HS, Varadavenkatesan T, *et al*., 2019. Photocatalytic zinc oxide nanoparticles synthesis using Peltophorum pterocarpum leaf extract and their characterization. Optik 185:248-55.

Pérez-Serrano J, Casado N and Rodriguez-Caabeiro F, 1994. The effects of albendazole and albendazole sulphoxide combination-therapy on *Echinococcus granulosus* in vitro. Int J parasitol 24:219-24.

Safawo T, Sandeep BV, Pola S, *et al*., 2018. Synthesis and characterization of zinc oxide nanoparticles using tuber extract of anchote (Coccinia abyssinica (Lam.) Cong.) for antimicrobial and antioxidant activity assessment. Open Nano 3:56-63.

Santhoshkumar J, Kumar SV and Rajeshkumar S, 2017. Synthesis of zinc oxide nanoparticles using plant leaf extract against urinary tract infection pathogen. Resource-Efficient Technologies 3:459-65.

Shakibaie M, Khalaf AK, Rashidipour M, *et al*., 2022. Effects of green synthesized zinc nanoparticles alone and along with albendazole against hydatid cyst protoscoleces. Ann Med Surg (Lond) 78:103746-6.

Shi H, Lei Y, Wang B, *et al*., 2016. Protoscolicidal effects of chenodeoxycholic acid on protoscoleces of Echinococcus granulosus. Exp parasitol 167:76-82.

Shnawa BH, Gorony SHM and Khalid KM, 2017. Efficacy of Cyperus rotundus rhizomes tubers extracts against protoscoleces of *Echinococcus granulosus*. World J Pharmac Res 6:1-23.

Shnawa BH, 2018. Advances in the use of nanoparticles as anti-cystic echinococcosis agents: a review article. J Pharmac Res Int 24:1-14.

Shnawa BH, Al-Ali SJ and Swar SO, 2021a. Nanoparticles as a new approach for treating hydatid cyst disease. Veterinary Pathobiology and Public Health; Unique Scientific Publishers: Faisalabad, Pakistan pp:180-9.

Shnawa BH, Hamad SM, Barzinjy AA, *et al*., 2021b. Scolicidal activity of biosynthesized zinc oxide nanoparticles by Mentha longifolia L. leaves against *Echinococcus granulosus* protoscolices. Emergent Mater pp:1-11.

Singh J, Kumar S, Alok A, *et al*., 2019. The potential of green synthesized zinc oxide nanoparticles as nutrient source for plant growth. J Clean Prod 214:1061-70.

Sirelkhatim A, Mahmud S, Seeni A, *et al*., 2015. Review on Zinc Oxide Nanoparticles: Antibacterial Activity and Toxicity Mechanism. Nano-Micro Lett 7:219-42.

Smyth J and Barrett N, 1980. Procedures for testing the viability of human hydatid cysts following surgical removal, especially after chemotherapy. Trans R Soc Trop Med Hyg 74:649-52.

Speakman SA, 2014. Estimating crystallite size using XRD. MIT Center for Materials Science and Engineering pp:3-8.

Taaca KLM and Vasquez MR, 2018. Hemocompatibility and cytocompatibility of pristine and plasma-treated silver-zeolite-chitosan composites. Appl Surf Sci 432:324-31.

Talam S, Karumuri SR and Gunnam N, 2012. Synthesis, Characterization, and Spectroscopic Properties of ZnO Nanoparticles. Int Sch Res Notices 2012:1-6.

Verma VC, Gangwar M and Nath G, 2014. Osmoregulatory and tegumental ultrastructural damages to protoscoleces of hydatid cysts *Echinococcus granulosus* induced by fungal endophytes. J parasit dis 38:432-9.

Whitesides GM, 2005. Nanoscience, Nanotechnology, and Chemistry. Small 1:172–9. doi:10.1002/smll.200400130

Zaheer T, Imran M, Pal K, Sajid MS, Abbas RZ, *et al*., 2021. Synthesis, characterization and acaricidal activity of green-mediated ZnO nanoparticles against *Hyalomma* ticks. J Mol Struct 1227:129652.